Efficiency of Active Three-Level and Five-Level NPC Inverters Compared to a Two-Level Inverter in a Vehicle

Efficiency of Active Three-Level and Five-Level NPC Inverters compared to a Two-Level Inverter in a Vehicle

Anton Kersten, Emma Grunditz, Torbjörn Thiringer
Chalmers University of Technology
Hörsalsvägen 11
Göteborg, Sweden
Email: kersten@chalmers.se, emma.grunditz@chalmers.se, torbjorn.thiringer@chalmers.se

September 2018

Keywords

≪Conduction losses≫, ≪Efficiency≫, ≪Electric vehicle≫, ≪IGBT≫, ≪MOSFET≫, ≪Multilevel converters≫, ≪Switching losses≫.

Abstract

This paper deals with a comparison of a standard two-level inverter, with a three-level and a five-level active neutral point clamped (ANPC) inverter for vehicle traction applications. The inverter efficiencies during different drive cycles are assessed and an efficiency enhancement of the multilevel inverters for partial loading and different drive cycle scenarios is found.

Introduction

In vehicle traction applications two-level inverter typologies are wide spread and vastly used, due to their maturity [1, 2]. However, emerging multilevel inverter typologies offer several advantages compared to common two-level inverters regarding efficiency [3], especially in partial load operation [4], reduction in common mode voltage and harmonic emissions. On the other hand, the disadvantages are an increased control effort and an increased system complexity. In [2] a generic power loss comparison of two-level and three-level PWM converters was conducted, where IGBT modules were applied. Here the switching losses of the three-level NPC converter are reduced and the conduction losses are increased, whereas the overall losses are reduced compared to the two-level inverter type. Moreover, as described in [4] the efficiency of IGBT modules under nominal load is usually higher than 97 %, whereas the overall drive cycle efficiency is unfortunately slightly lower due to the variable load. In contrast, when partly loaded, MOSFETs can have a higher efficiency than IGBTs. For this reason it can be reasonable to utilize low voltage MOSFETs in multilevel inverters for vehicle applications. Within this paper a comparison of a two-level inverter, utilizing IGBTs, with a three and five-level ANPC converter using low voltage MOSFETs is carried out with respect to several drive cycle operation scenarios.

Multilevel Inverter

In general, the output of a classical two-level inverter is alternatingly switched between two voltage levels supplied by the voltage source, while semiconductor switches as MOSFETs and IGBTS are used to attain a high switching frequency. If the switched output voltage is applied to an inductive load, the resulting output current is sinusoidally shaped, with a small ripple component. In a multilevel inverter the output voltage is switched between several voltage levels, which is supplied by several voltage sources connected in series. Consequently, the output voltage can be formed by various voltage levels described

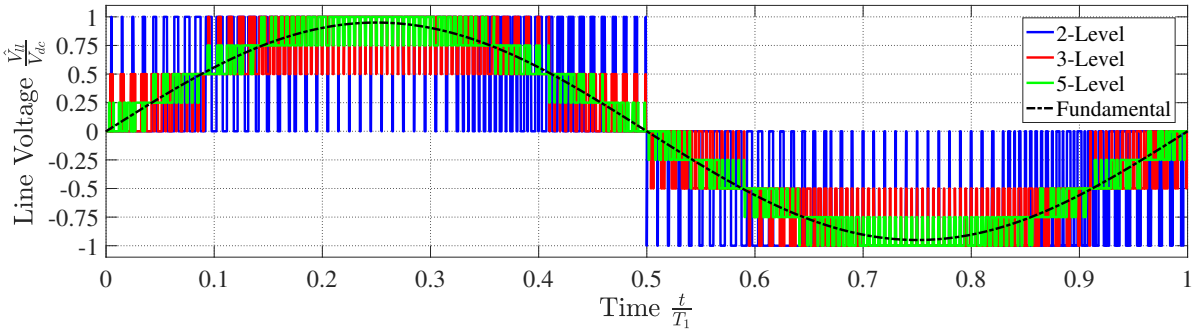

(a) Output voltage

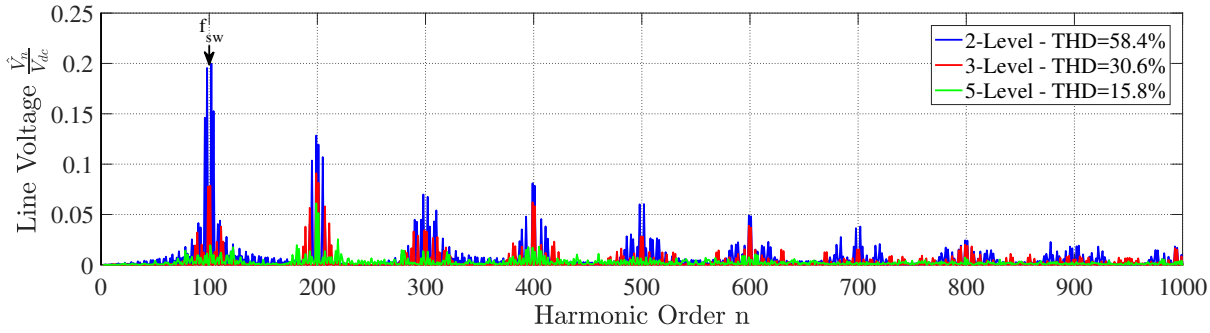

(b) Output voltage harmonics

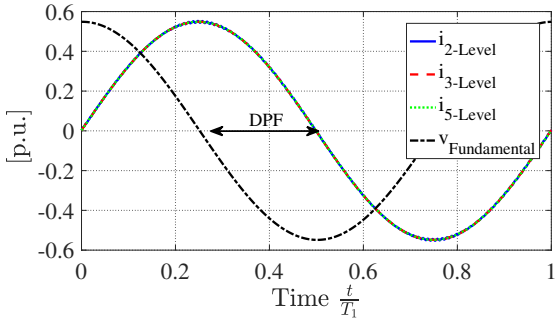

(c) Phase current

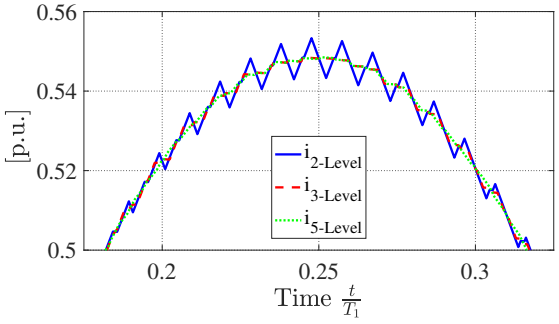

(d) Current ripple

Fig. 1: Multilevel inverter waveforms and voltage harmonics.

as $\pm\frac{V_{DC}}{n-1}i$, with n as the number of levels and $i = 0; 1; \ldots \frac{n-1}{2}$. Fig. 1 shows the line voltage and the corresponding harmonic spectra for inverters with different number of levels, using space vector modulation, utilizing the same sample/update time. It can be stated that the THD of the voltage is reduced from 58.4 % to 15.8 %, when using a five-level inverter compared to a common two-level inverter. Furthermore, the resulting currents, when applied to an RL-load, can be seen in Fig. 1c, while a more detailed view is depicted in Fig. 1d. The current THD is generally quite low, about 1 %, when using a switching frequency several times higher than the fundamental. Nevertheless, the current ripple is reduced with the increasing number of switching-levels, which in turn reduces the electromagnetic interferences and the torque ripple in motor applications. However, when controlling a motor, the switching frequency of a multilevel inverter cannot be necessarily reduced, since controllability might be lost at high fundamental frequencies. Therefore, selective harmonic elimination is a favoured switching technique for multilevel inverters, which in turn makes a direct comparison difficult.

Active Neutral Point Clamped (ANPC) Inverter

Neutral point clamped (NPC) inverter topologies are used in connection with a low number of voltage levels, commonly for three or five levels, because the number of switching elements is increasing expo-

nentially with the number of levels. Normally, diodes are used to clamp the voltage to one or several intermediate voltage levels. In an active neutral point clamped, ANPC, inverter, these diodes are replaced by MOSFETs, which consequently reduce the conduction losses. Fig. 2 shows the inverter topologies, considered in this article's comparison. The index of the switches' gate signal is referring to the voltage level, during which the switch is conducting. For example, if the second voltage level shall be activated, all switches containing the number 2 in their index should be activated.

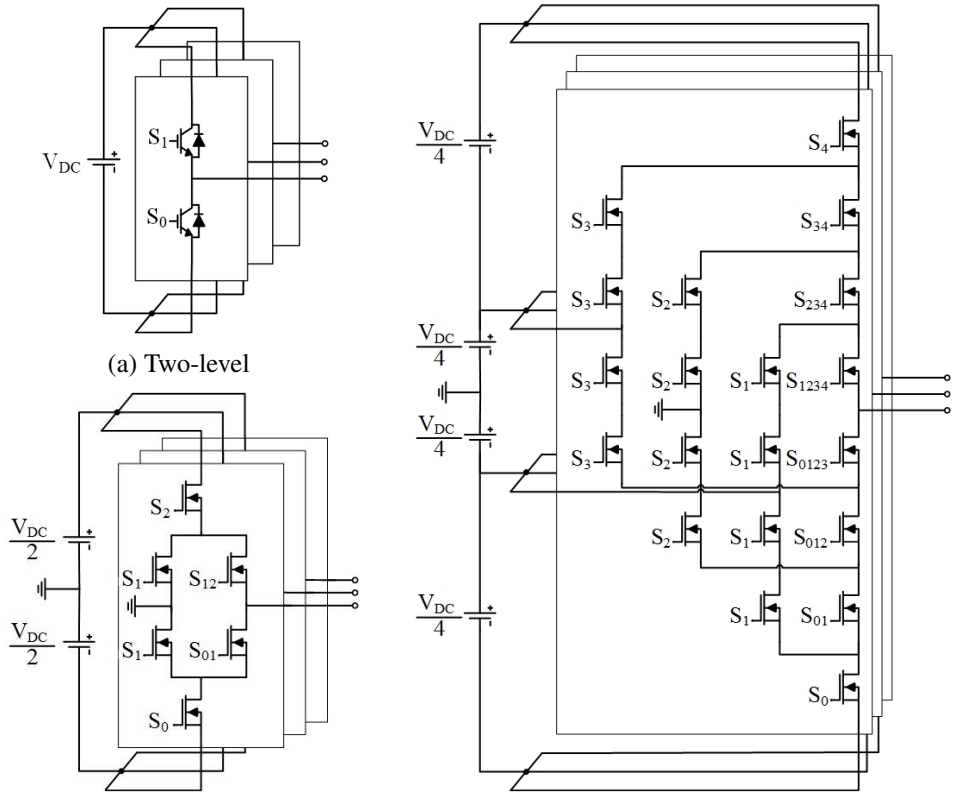

(a) Two-level

(b) Three-level

(c) Five-level

Fig. 2: Two (a), three (b) and five-level (c) ANPC multilevel inverter topologies.

Thermal Modeling

To determine the temperature dependent losses in the power electronic switches, a software based lookup table approach can be used, that utilizes a linear interpolation between temperature specific lookup tables. Here, the conduction loss is implemented as a voltage drop across the semiconductor switch as a function of the current, as can be seen for instance in Fig. 3a. In this connection, the product of voltage and current yields the instantaneous conduction loss. IGBTs with anti-parallel diodes are minority carrier devices, which typically have a diode characteristic in forward and reverse conduction. On the contrary, MOSFETs, as majority carrier devices, have a resistive forward characteristic, which also can be utilized in reverse conduction, when switched on. This in turn results in the parallel conduction of the n-channel and the body or package diode [5]. Hereby, the conduction losses of the MOSFETs at partial loading are typically reduced compared to IGBTs. The switching losses are modeled as a lookup table representing the dissipated energy for a switching event with a certain blocking voltage and device current, as depicted in Fig. 3b. The lookup tables can be created according to [6] and [7], while the IGBTs' switching losses are scaled according to

$$E_{on+off} = E_{ref} \cdot \left(\frac{i}{i_{ref}}\right)^{K_i} \left(\frac{V_{DC}}{V_{ref}}\right)^{K_v} \quad . \tag{1}$$

The constants K_v and K_i are typically 1 and 1.3 to 1.4, respectively, for the IGBT's switch and 0.6 and 0.6 for the IGBT's anti parallel diode, respectively [8]. Next, the losses are used to calculate the switches' average junction temperatures. Fig. 3c shows a simple zero order thermal network, assuming evenly distributed losses and N discrete switches. All time constants are neglected thus the steady state temperature is reached instantly. The coolant's temperature can be controlled by its flow velocity within a range from 65 °C to 85 °C [8].

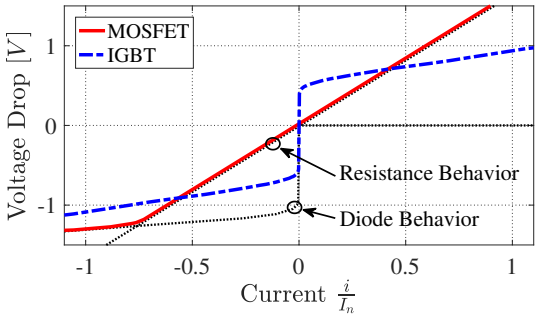

(a) Forward and reverse voltage drop

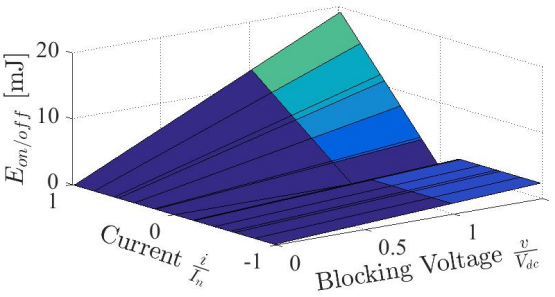

(b) Switching energy

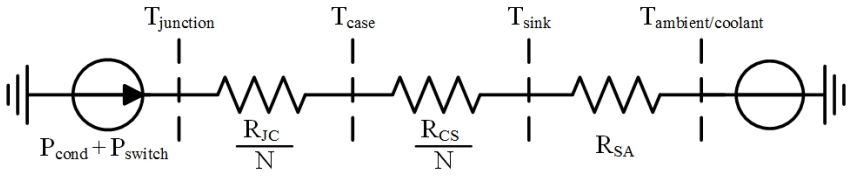

(c) Thermal model

Fig. 3: Conduction loss (a), switching loss (b) and thermal modeling (c).

Motor and Vehicle Dynamics

The governing equations of an interior permanent magnet synchronous machine's (IPM) stator voltages in dq-reference can be expressed as

$$v_d = R_s i_d + L_d \frac{di_d}{dt} + n_p \omega_m L_q i_q \quad \text{and} \tag{2}$$

$$v_q = R_s i_q + L_q \frac{di_d}{dt} + n_p \omega_m (L_d i_d + \psi_m) \quad . \tag{3}$$

Following upon this, the resulting electromagnetic torque of the motor is dependent on the inductance difference in dq-reference and the magnetic constant, as can be described as

$$T_{electrical} = \frac{3n_p}{2}[(L_d - L_q) i_d i_q + \psi_m i_q] \quad , \tag{4}$$

while the gearbox ratio and the gearbox's efficiency are considered as

$$T_{electrical} = T_{motor} = \frac{T_{wheel}}{\eta_G G_r} \quad \text{and} \tag{5}$$

$$\frac{\omega_{electrical}}{n_p} = \omega_{motor} = \omega_{wheel} G_r \quad . \tag{6}$$

The mechanical system of a vehicle's drive train can be modeled as a simple first order system

$$J \frac{d\omega_{wheel}}{dt} = T_{electrical} - T_{wheel} \quad , \tag{7}$$

where a steady state velocity is reached at the torque equilibrium. Here, the wheel's torque can be calculated by the product of the sum of forces acting on the car and the wheels' radius as

$$T_{wheel} = r_{wheel} F_{net} \quad . \tag{8}$$

The overall forces acting on the vehicle in longitudinal direction consists of the sum of the rolling/friction resistance, aero dynamic drag, road gradient and acceleration force as

$$F_{net} = F_{rolling} + F_{aero} + F_{gradient} + F_{acceleration} \quad , \tag{9}$$

whereas the single forces can be calculated according to

$$F_{acceleration} = m_{veh}\, a \quad , \tag{10}$$

$$F_{airdrag} = 0.5\, \rho_{air}\, C_d\, v^2\, A \quad , \tag{11}$$

$$F_{rolling} = m_{veh}\, g\, C_r\, cos(\alpha) \quad \text{and} \tag{12}$$

$$F_{gradient} = m_{veh}\, g\, sin(\alpha) \quad . \tag{13}$$

Here, the acceleration and the gradient force can be positive or negative. To perform a drive cycle analysis, the operating points of the motor, and consequently of the inverter, can be determined from the corresponding vehicle speed and acceleration profile, as can be seen for instance in Fig. 4.

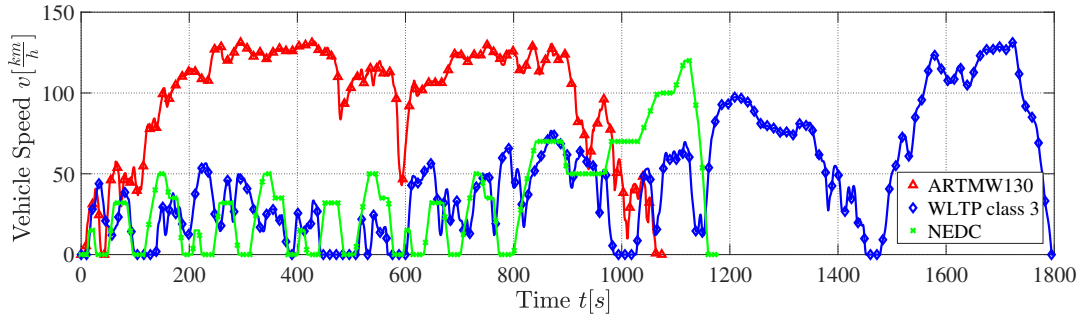

(a) Drive cycles

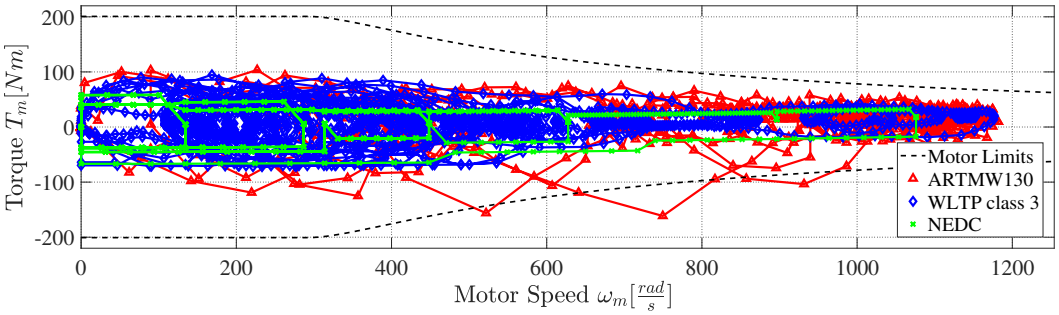

(b) Motor load

Fig. 4: Drive cycles (a) and the corresponding motor operating points (b).

Simulation Model and Case Setups

All simulations were conducted using MATLAB Simulink and Plexim's PLECS. The simulation model is divided into two subsequent tasks, the loss calculation of the inverter and the drive cycle analysis, as schematically depicted in Fig. 5. In the first part, a number of 3D-loss maps of the inverter are created according to the motor operating points and the junction temperatures, as can be seen in Fig. 5a. For each operating point within the torque boundaries the corresponding currents in direct and quadrature axis are calculated according to the governing equations of the IPM, while considering MTPA and flux weakening with respect of current and voltage constraints [9, 10] . Following this, a PI-regulator is used to control the motor currents, while the motor speed is fixed. Finally, at steady state, the conduction and switching losses of the inverter are obtained. During the second part, the drive cycle analysis, the motor operating points are calculated by the vehicle model according to (8)-(13). Subsequently, the losses are read from the previously created loss lookup table. These are input to the simple zero order thermal model with a fixed coolant temperature. The obtained temperature is then feed forwarded in an algebraic loop as a parameter of the losses' lookup table.

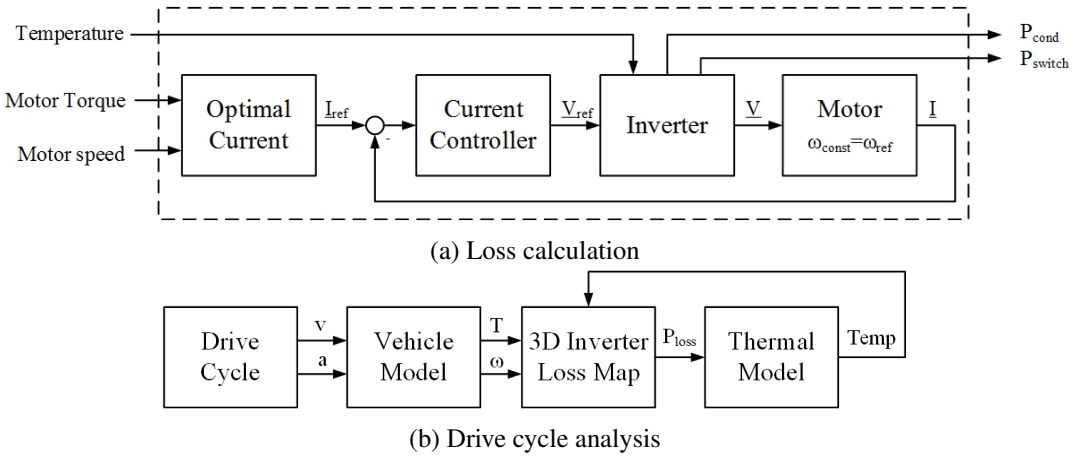

Fig. 5: Simulation model including loss map calculation (a) and drive cycle analysis (b).

The vehicle and motor parameters of the used simulation setup are depicted in Table I. These are inspired from [8, 11] and are intended to represent a small passenger car with a 84 kW rated motor.

Table I: Setup parameters

(a) Vehicle

	Value	Unit
Vehicle mass m_{veh}	1500	kg
Occupant weight m_{occ}	75	kg
Frontal area A	2.2	m^2
Drag cofficient C_d	0.28	m^2
Rolling resistance C_r	0.009	
Wheel radius r_{wheel}	0.316	m
Gear box ratio G_r	10.2	
Gearbox efficiency η_G	95	%
Top speed v_{max}	140	km/h

(b) Motor

	Value	Unit
Stator resistance R_s	20	mΩ
D-axis inductance L_d	250	µH
Q-axis inductance L_q	700	µH
Flux constant ψ_m	75	mWb
Pole pairs n_p	4	
Max torque T_{max}	200	N m
Max phase current I_{RMS}	190	A
Max phase voltage V_{RMS}	200	A
Max speed n	12000	rpm

For the simulated drive train a DC-link of V_{DC}= 400 V is assumed. Therefore the blocking capability of the semiconductor switches should withstand overvoltages, caused by the switching events, of 50 % of the DC link's voltage. For this reason 650 V rated IGBTs are commonly applied for two-level inverters operating with V_{DC}= 400 V, while the switching frequency is typically set to f_{sw}=10 kHz for vehicle applications. The temperature of the coolant is set to 75 °C.

Table II depicts the semiconductor switches used for the corresponding inverter setups. The chosen IGBT module is a universal product, which can be found in various drive applications for different motor power ratings. To meet the current rating of the setup motor, 6 and 3 of the low voltage MOSFETs must be placed in parallel for each switch depicted in Fig. 2b and Fig. 2c, respectively. The overall resulting number of discrete elements N is large. These are intended to be placed in a single large module in the future, whereby the inverter size could be decreased. For instance, the IGBT module has a volume of 442.8 cm^3, whereas the volume of the five-level inverter's MOSFET-package times N equals 68.0 cm^3.

Table II: Inverter parameters.

Inverter	Switch	Vendor	Type	$V_{blocking}$	I_{max}	N	Unit Price[1]
Two-level	FS600R07A2E3	Infineon	IGBT	650 V	600 A	6	504.39 €[2]
Three-level ANPC	IRFP4868PbF	Infineon	MOSFET	300 V	49 A	108	2.59 €
Five-level ANPC	IPB044N15N5	Infineon	MOSFET	150 V	123 A	180	2.83 €

[1] For purchase of at least 1000 units, [2] price for entire IGBT module

Drive Cycle Performance

The first simulation part, depicted in Fig. 5a, is used to obtain the semiconductors' losses in all three inverter setups over a temperature interval from 70 °C to 100 °C, with a stepsize of 10 K. In this manner the full temperature range of the semiconductor switches is covered. As an example, Fig. 6 depicts the efficiency maps, calculated from the obtained loss maps at a junction temperature of 80 °C.

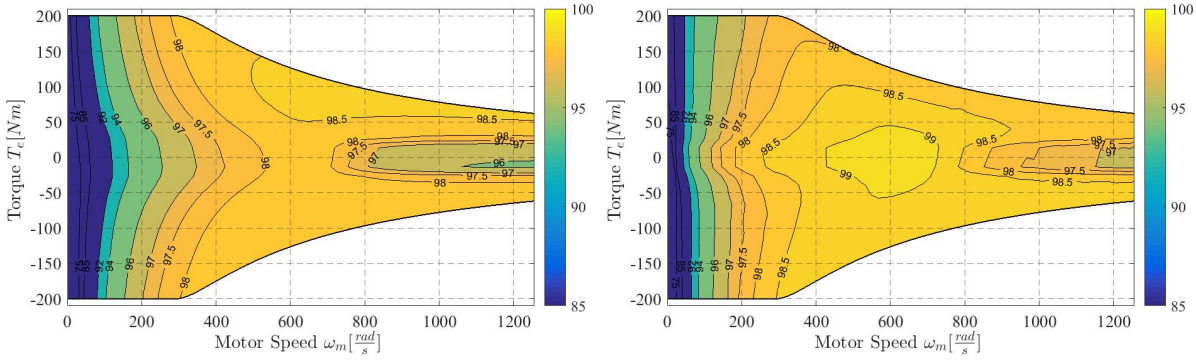

(a) Two-level - IGBT

(b) Three-level ANPC - MOSFET

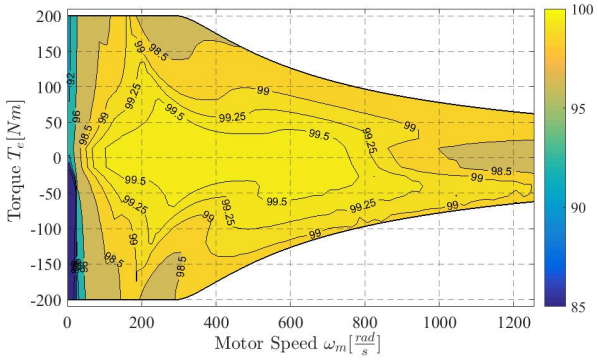

(c) Five-level ANPC - MOSFET

Fig. 6: Motor efficiency maps for the two-level (a), three-level (b) and five-level (c) setup at $T_j = 80\,°\mathrm{C}$.

At generator and partial load operation, the MOSFET multilevel converters have an enhanced efficiency in comparison to the two-level IGBT converter. This is especially due to the low conduction losses at partial loading, as depicted in Fig. 3a. At higher load, until rated load operation, the two-level inverter is more efficient than the three-level solution. Exactly at rated motor load and high speed operation, the two-level IGBT inverter has a similar efficiency as the five-level MOSFET inverter. Fig. 7 emphasizes

the particular beneficial operating regions, where the multilevel inverter solutions achieve efficiency enhancements in comparison to the common two-level IGBT inverter.

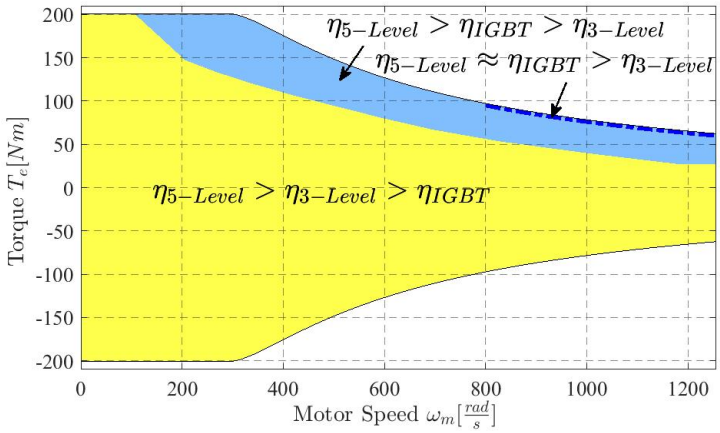

Fig. 7: Comparison of the inverter efficiencies at $T_j = 80\,°\text{C}$.

Therefore, to determine the actual drive cycle performance, the second simulation part, depicted in Fig. 5b, is used. As an example, Fig. 8 shows the drive cycle performance for the WLTP class 3 drive cycle. Energy consumption, energy loss and the junction temperatures during the cycle are depicted graphically, and the final results are also in Table III.

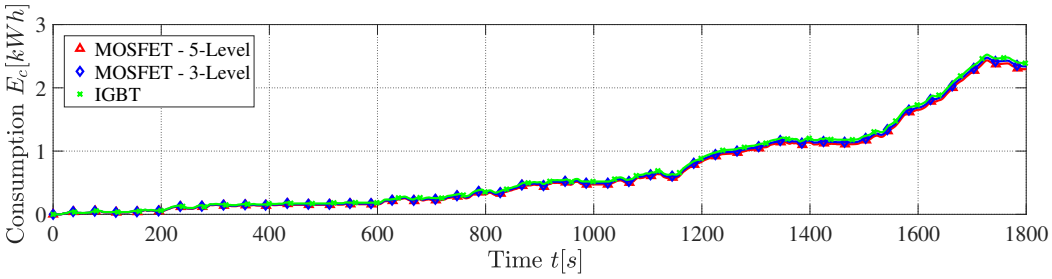

(a) Absolute energy consumption

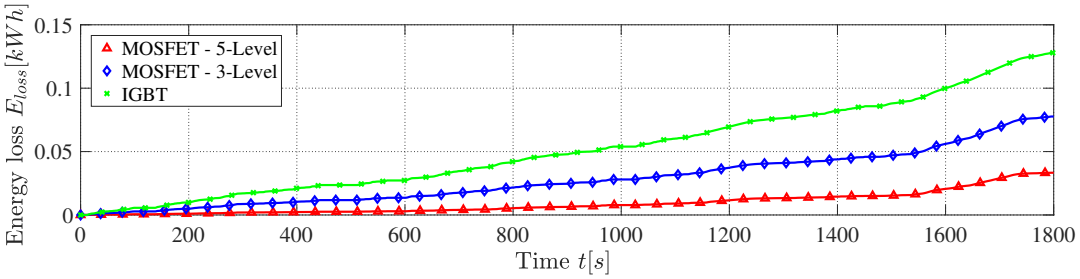

(b) Total inverter losses

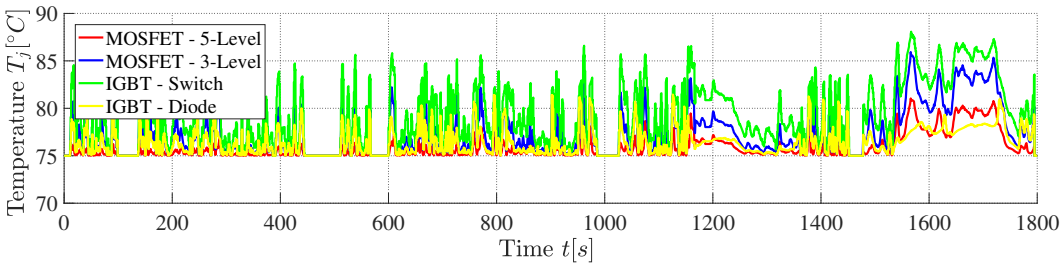

(c) Junction temperatures

Fig. 8: WLTP class 3 drive cycle performance.

During the WLTP class 3 cycle the three-level and five-level inverter setups reducing the energy loss by 39 % and 74 %, which in turn results in a reduced energy consumption of 2 % and 4 %, respectively. Furthermore, it can be seen that the temperatures vary within a range from 75 °C, the coolant's temperature, and maximum of 88 °C for the two-level IGBT inverter, which is not critical. Considering the drive cycle performance during other cycles, it can be seen that a similar result is obtained for the city cycles with a slow acceleration and speed variation. Here, the energy loss is reduced by up to 84.2 %, which in turn reduces the energy consumption by up to 7.2 %. Regarding the ARTMW 130, which has a higher load demand and a fast speed and high acceleration variation, the energy consumption is reduced by just 1.8 % when using the five-level MOSFET inverter.

Table III: Drive cycle performance

(a) WLTP Class 3

	IGBT	3-Level ANPC	Δ_1	5-Level ANPC	Δ_2
Energy loss E_{Loss}	0.128 kWh	0.078 kWh	-39.0 %	0.033 kWh	-74.2 %
Rel. consumption $\frac{E_c}{100\,\mathrm{km}}$	10.27 kWh	10.06 kWh	-2.0 %	9.86 kWh	-4.0 %
Temperature T_{j-max}	88.1 °C	85.9 °C	-2.17 K	81.0 °C	-7.1 K

(b) NEDC

	IGBT	3-Level ANPC	Δ_1	5-Level ANPC	Δ_2
Energy loss E_{Loss}	0.0615 kWh	0.033 kWh	-46.3 %	0.010 kWh	-83.5 %
Rel. consumption $\frac{E_c}{100\,\mathrm{km}}$	8.62 kWh	8.38 kWh	-2.8 %	8.19 kWh	-5.0 %
Temperature T_{j-max}	86.8 °C	84.7 °C	-2.1 K	80.3 °C	-6.5 K

(c) ARTMW 130

	IGBT	3-Level ANPC	Δ_1	5-Level ANPC	Δ_2
Energy loss E_{Loss}	0.156 kWh	0.123 kWh	-21.12 %	0.073 kWh	-41.7 %
Rel. consumption $\frac{E_c}{100\,\mathrm{km}}$	15.33 kWh	15.22 kWh	-0.7 %	15.05 kWh	-1.8 %
Temperature T_{j-max}	91.2 °C	90.7 °C	-0.5 K	86.2 °C	-5.0 K

(d) FTP - 75

	IGBT	3-Level ANPC	Δ_1	5-Level ANPC	Δ_2
Energy loss E_{Loss}	0.114 kWh	0.0625 kWh	-55.2 %	0.018 kWh	-84.2 %
Rel. consumption $\frac{E_c}{100\,\mathrm{km}}$	7.53 kWh	7.24 kWh	-3.8 %	6.99 kWh	-7.2 %
Temperature T_{j-max}	86.1 °C	82.6 °C	-3.5 K	79.0 °C	-7.1 K

(e) HWFET

	IGBT	3-Level ANPC	Δ_1	5-Level ANPC	Δ_2
Energy loss E_{Loss}	0.052 kWh	0.028 kWh	-46.3 %	0.0123 kWh	-76.4 %
Rel. consumption $\frac{E_c}{100\,\mathrm{km}}$	10.08 kWh	9.94 kWh	-1.4 %	9.85 kWh	-2.3 %
Temperature T_{j-max}	85.0 °C	81.3 °C	-3.7 K	77.9 °C	-7.1 K

Conclusion

From the presented investigation it is seen that the three-level and five-level inverters, utilizing low voltage MOSFETs, show a high potential for energy savings compared to a classical two-level IGBT inverter. Especially at partial loading, as typical for city cycles, the low voltage MOSFETs attain a beneficial energy saving. At high speed and rated load operation, the potential for energy savings is reduced. However, the analysis just focused on the efficiency enhancement potentials, whereas the power density and system realization were neglected. The number of discrete switches, as depicted in Table II, might result in a system with a lowered power density, due to an increased system complexity compared to the two-level inverter setups. In the future, the switches should be optimized for low blocking voltages and higher current capacities. Furthermore, these should be placed in a single large module.

References

[1] S. Brueske, S. Walz, M. Liserre, and F. W. Fuchs, "Loss balancing of three-level inverters in electric vehicles for low speed operation," in *2016 18th European Conference on Power Electronics and Applications (EPE'16 ECCE Europe)*, Sept 2016, pp. 1–10.

[2] P. Alemi and D. C. Lee, "Power loss comparison in two- and three-level pwm converters," in *8th International Conference on Power Electronics - ECCE Asia*, May 2011, pp. 1452–1457.

[3] M. Schweizer, T. Friedli, and J. W. Kolar, "Comparative evaluation of advanced three-phase three-level inverter/converter topologies against two-level systems," *IEEE Transactions on Industrial Electronics*, vol. 60, no. 12, pp. 5515–5527, Dec 2013.

[4] F. Chang, O. Ilina, O. Hegazi, L. Voss, and M. Lienkamp, "Adopting mosfet multilevel inverters to improve the partial load efficiency of electric vehicles," in *2017 19th European Conference on Power Electronics and Applications (EPE'17 ECCE Europe)*, Sept 2017, pp. P.1–P.13.

[5] A. Acquaviva and T. Thiringer, "Energy efficiency of a sic mosfet propulsion inverter accounting for the mosfet's reverse conduction and the blanking time," in *2017 19th European Conference on Power Electronics and Applications (EPE'17 ECCE Europe)*, Sept 2017, pp. P.1–P.9.

[6] Infineon technologies AG, "Mosfet power losses calculation using the datasheet parameters," http://application-notes.digchip.com/070/70-41484.pdf, (Accessed on 05/16/2018).

[7] ——, "Igbt power losses calculation using the data-sheet parameters," https://www.element14.com/community/docs/DOC-20553/l/igbt-power-losses-calculation-using-the-data-sheet-parameters, (Accessed on 05/16/2018).

[8] E. Grunditz, *Design and Assessment of Battery Electric Vehicle Powertrain, with Respect to Performance, Energy Consumption and Electric Motor Thermal Capability*, ser. Doktorsavhandlingar vid Chalmers tekniska högskola. Ny serie, no:. Institutionen för energi och miljö, Elteknik, Chalmers tekniska högskola,, 2016, 229.

[9] S. Halder, S. P. Srivastava, and P. Agarwal, "Flux weakening control algorithm with mtpa control of pmsm drive," in *2014 IEEE 6th India International Conference on Power Electronics (IICPE)*, Dec 2014, pp. 1–5.

[10] J. Bonifacio and R. Kennel, "Online maximum torque per ampere control of interior permanent magnet synchronous machines (ipmsm) for automotive applications," in *8th IET International Conference on Power Electronics, Machines and Drives (PEMD 2016)*, April 2016, pp. 1–5.

[11] O. Josefsson, *Investigation of a Multilevel Inverter for Electric Vehicle Applications*, ser. Doktorsavhandlingar vid Chalmers tekniska högskola. Ny serie, no:. Institutionen för energi och miljö, Elteknik, Chalmers tekniska högskola,, 2015, 146.